Nanorod Self-Assembly

DOI: 10.1002/anie.201004915

Self-Assembly of Single-Tip Metal–Semiconductor Nanorods in Selective Solvents**

*Nana Zhao, Jemma Vickery, Gerald Guerin, Jai Il Park, Mitchell A. Winnik, and Eugenia Kumacheva**

Studies on the synthesis, properties and applications of hybrid inorganic nanoparticles constitute a frontier area of research in nanoscience.[1,2] In particular, metal–semiconductor nanorods (NRs) have the following useful features: 1) light-induced charge separation between the semiconductor and metal segments,[3] which is promising in photovoltaic applications; 2) plasmonic and local-field enhancement effects leading to increased absorbance and potentially to improved light harvesting;[4–6] 3) improved electrical contact in photovoltaic devices,[7] owing to the presence of metal tips that serve as anchor points;[5,7–9] and 4) the propensity to form ordered arrays in selective solvents, which is governed by the different solubilities of the ligands stabilizing the metal and semiconductor components.[10–14] The last feature is important for future integration of NRs in functional devices.

Solution-based generation of lattices of side-by-side aligned CdSe NRs with two symmetric Au tips has been reported.[12] On the other hand, standing arrays of single-tip Au–semiconductor NRs are more promising for applications in the fabrication of photovoltaic devices, because they enable more efficient charge separation (holes and electrons) to two opposite electrodes. Since the first report on the synthesis of single-tip Au–semiconductor NRs,[15,16] two groups have reported well-organized structures thereof. Tip-to-tip assembly of Au–CdSe@CdS NRs was triggered by adding iodine to the NR solution in order to displace ligands on the Au tips and induce attraction between them.[10] Standing arrays of side-by-side aligned Au-CdS NRs were produced by spin-casting a solution of AuCl on the superlattice of perpendicularly aligned CdS NRs and subsequently reducing Au^{I} to Au^{0} with dodecylamine, thereby synthesizing a single Au tip on each NR.[7] No systematic study of controllable tip-to-tip and side-by-side solution-based assembly of single-tip Au–CdSe NRs has been reported.

Here we report on a systematic study of solution-based self-assembly of single-tip Au–CdSe NRs by using transmission electron microscopy (TEM) and static and dynamic light scattering (SLS and DLS, respectively). We exploited the resemblance between Au–CdSe NRs and low molecular weight rigid amphiphilic molecules. We conducted two distinct series of experiments, in which the assembly of NRs was governed by the quality of the solvent for the ligands coating the Au tips or the long CdSe sides of NRs (Figure 1).

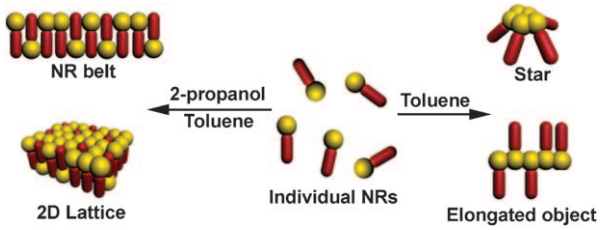

Figure 1. Solution-based self-assembly of single-tip Au–CdSe NRs.

The as-synthesized NRs show good stability in nonpolar solvents such as toluene. Due to gradual removal of the ligands coating the Au tips, in the absence of external perturbation the NRs underwent tip-to-tip association, in order to minimize interactions between the nonpolar solvent and the polar Au tips. This type of assembly led to formation of starlike entities and a smaller number of elongated objects.

Addition of a polar solvent to the solution of NRs in toluene reduced the solvent quality for the nonpolar ligands capping the CdSe segments. To minimize interactions between the solvent and the ligands, the NRs organized in a side-by-side fashion to form belts or large planar two-dimensional lattices (membranes). This self-assembly mode was controlled by two factors: the relative volume fractions of the Au and CdSe segments, and the quality of solvent for each of them. Formation of the self-assembled structures was "mapped" onto a phaselike diagram.

We synthesized three types of single-tip Au–CdSe NRs with varying volumes of the CdSe segment. The Au component of the NRs was coated with didodecyldimethylammonium bromide (DDAB) and dodecylamine (DDA), which we refer to as tip ligands (TLs).[17] The CdSe segment was stabilized with C_{12} thiol side ligands (SLs).

Table 1 shows the structural characteristics of the NRs used in the present work. In all three samples, the Au tips had a spherical shape and an average diameter of 5.3–5.4 nm. The average length and width of the CdSe segment varied from 7.5 to 27.5 nm and from 3.0 to 4.1 nm, respectively. The volume fraction of the CdSe component A_{CdSe} ranged from 0.4 to 0.8. Because of the density difference between the two compo-

[*] Dr. N. Zhao, Dr. J. Vickery, Dr. G. Guerin, J. I. Park, Prof. Dr. M. A. Winnik, Prof. Dr. E. Kumacheva
Department of Chemistry, University of Toronto
80 Saint George Street, Toronto M5S 3H6, Ontario (Canada)
Fax: (+1) 416-978-3576
E-mail: ekumache@chem.utoronto.ca

[**] E.K. thanks the Canada Research Chair support (NSERC Canada). Assistance of Dr. N. Coombs and Ilya Gourevich in the SEM and TEM imaging is appreciated. The authors thank M. Soleimani for assistance in the Monte Carlo simulations.

Supporting information for this article is available on the WWW under http://dx.doi.org/10.1002/anie.201004915.

Table 1: Dimensions of the Au and CdSe segments in the NRs.

Sample[a]	Au tip	CdSe segment		A_{CdSe}[b]	R_g[c] [nm]
	Average diameter [nm]	Average length [nm]	Average width [nm]		
1	5.3 ± 0.5	7.5 ± 0.8	3.0 ± 0.4	0.4	3.2
2	5.3 ± 0.4	14.8 ± 2.0	3.1 ± 0.5	0.6	5.5
3	5.4 ± 0.4	27.5 ± 2.5	4.1 ± 0.8	0.8	10.3

[a] The white dot indicates the locus of the center of mass for each type of NR. The calculations of the loci of the centers of mass and the radii of gyration R_g of the NRs are given in Supporting Information. [b] $A_{CdSe} = V_{CdSe}/(V_{CdSe}+V_{Au})$. [c] In the calculations of R_g, the contribution of ligands was ignored.

nents, the loci of the centers of mass of the NRs were heavily weighted by the Au segment.

First we studied tip-to-tip assembly of NRs. The as-synthesized NRs exhibited colloidal solubility in toluene. Over time these structures began to aggregate via the Au tips. We ascribe this self-assembly to growing attraction between the Au tips, induced by gradual replacement of TLs by Br^- ions, which were introduced with DDAB. This in agreement with the work of Manna et al.,[10] who demonstrated that I_2 triggers tip-to-tip self-assembly of single-tip Au–CdSe@CdS NRs by replacing TLs on the surface of the Au segment.

Figure 2 shows structures generated by tip-to-tip assembly ($A_{CdSe} = 0.6$). After 6 h of incubation mostly bipods and tripods formed, which coexisted with a large number of

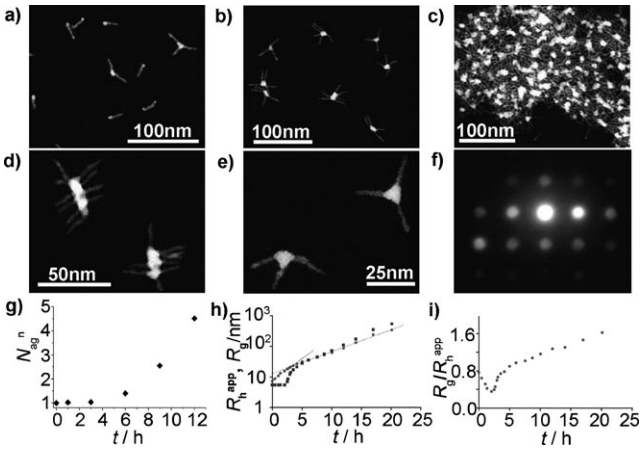

Figure 2. a–c) Dark-field TEM images of starlike structures of NRs with $A_{CdSe} = 0.6$ after incubation in toluene at a concentration of 0.2 mg mL^{-1} for 6, 12, and 18 h, respectively. High-resolution TEM images of elongated objects (d) after NR incubation in toluene for 12 h and of tripods (e) obtained as in a). f) Electron diffraction of fused Au core in a star obtained as in a). g) Variation of the average aggregation number N_{ag}^n (calculated from TEM-image analysis), plotted as a function of time of solution incubation. For each time interval about 700 NRs were analyzed. h) Variation in the apparent hydrodynamic radius R_h^{app} (circles) and radius of gyration R_g (squares), plotted as a function of self-assembly time from DLS measurements (0.1 mg mL^{-1}).The dashed lines emphasize the change in slope of the variation in R_h^{app} prior to and after 5 h. i) Variation in ratio R_g/R_h^{app} with incubation time.

individual NRs (Figure 2a). After 12 h, starlike multipods were the majority structure (Figure 2b). By 18 h, the stars themselves began to aggregate (Figure 2c). Over intermediate periods of time (e.g., 12 h), we found approximately 5% of elongated objects coexisting with stars (Figure 2d). High-magnification imaging revealed that the central Au core of the stars was formed by fused Au tips (Figure 2e). The CdSe arms of the stars stood on the substrate in a spiderlike manner. Approximately 60% of the stars were characterized by a single-crystalline lattice in the fused Au core (Figure 2f).

We analyzed TEM images to calculate the number-average aggregation number ($N_{ag}^n = \Sigma n_i N_i / \Sigma n_i$) of the stars. Here N_i is the number of NRs in the star, and n_i is the number of stars with aggregation number N_i. Figure 2g shows the variation in N_{ag}^n with incubation time up to 12 h. Following a lag period of about 4.5 h, N_{ag}^n increased to 4.5 at 12 h. At longer times the stars themselves began to aggregate, and we were unable to calculate N_{ag}^n values from TEM images.

In light-scattering experiments, association of NRs in toluene occurred with a lag time that depended both on the structure and on the concentration of the NRs. For example, for the NRs with $A_{CdSe} = 0.4$ this period was up to days, whereas the NRs with $A_{CdSe} = 0.6$ and $A_{CdSe} = 0.8$ started to self-assemble in hours. On dilution, the sample with $A_{CdSe} = 0.6$ exhibited a shorter lag time of about 1 h. A different rate of NR self-assembly was the main difference between the TEM-imaging (Figure 2g) and light-scattering experiments (see Supporting Information).

In the corresponding light-scattering experiments the solutions of NRs in toluene were diluted to a concentration of 0.1 mg mL^{-1}. Self-assembly was characterized by the changes in the apparent hydrodynamic radius R_h^{app} and the radius of gyration R_g (Figure 2h,i), as well as the weight-average aggregation number N_{ag}^w (see Supporting Information).

Figure 2h shows semi-logarithmic plots of the variation of R_h^{app} and R_g as a function of time. Based on the change in R_h^{app}, the self-assembly began within 1 h after sample preparation, but little change occurred in R_g. The plots of intensity versus scattering angle show very small slopes (Supporting Information), and while there is uncertainty in the absolute magnitude of these small values of R_g, it is clear that they did not increase over the first 3 h of the self-assembly process. This unusual behavior is a consequence of the asymmetric nature of the NRs (the densities of Au and CdSe are 19.3 and 5.8 g cm^{-3}, respectively). Tip-to-tip association shifts the center of mass of the dimer and trimer into the Au domain, and the high density of Au compared to CdSe means that the magnitude of R_g is heavily weighted by the Au segment. In contrast, the CdSe arms of the stars contribute to R_h^{app}, which makes R_h^{app} sensitive to the early stages of self-assembly. We emphasized this point by plotting R_g/R_h^{app} versus time (Figure 2i). In this plot, R_g/R_h^{app} passes through a minimum at about 2.5 h, which corresponds to the onset of the increase in R_g in Figure 2h. Low values of R_g/R_h^{app} are characteristic of systems in which the mass is concentrated in the central core, surrounded by lighter entities that protrude into the solution and reduce the diffusion rate.[18] The second self-assembly stage was accompanied by a rapid increase in R_g, which reached 550 nm after

20 h (Figure 2h). For these large assemblies N_{ag}^{w} reaches values as large as 1000 after 20 h (see Supporting Information). The increased ratio R_g/R_h^{app} is also consistent with the formation of large aggregates, such as that seen in the TEM image in Figure 2c.

Next, we examined side-by-side assembly of NRs. Figure 3 shows representative images of self-assembled NR structures in toluene/2-propanol. Qualitatively similar results were obtained for NRs in DMF/toluene (Supporting Information). The experimental variables in this process were the volume fraction of 2-propanol (C_I in vol%) and the volume fraction A_{CdSe} of the CdSe component.

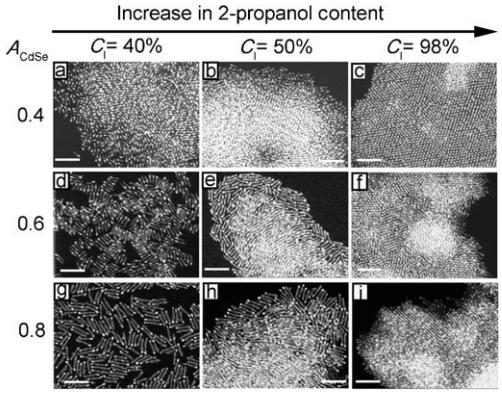

Figure 3. Dark-field TEM images of single-tip Au–CdSe NRs incubated for 4 h in 2-propanol/toluene with different volume fractions of 2-propanol C_I [vol%]. From top to bottom A_{CdSe} indicates the volume fraction of CdSe in the single-tip Au–CdSe NRs. Scale bar: 50 nm. Concentration of NRs in the final solution: a–f) 0.8, g–i) 1.0 mg mL^{-1}.

By analyzing the TEM images, we mapped self-assembly of the NRs in a phaselike diagram in the C_I–A_{CdSe} parameter space (Figure 4). We observed three types of structures: individual NRs, planar beltlike structures one NR wide, which we call "belts", and large two-dimensional (2D) membrane-like aggregates that we refer to as "lattices".

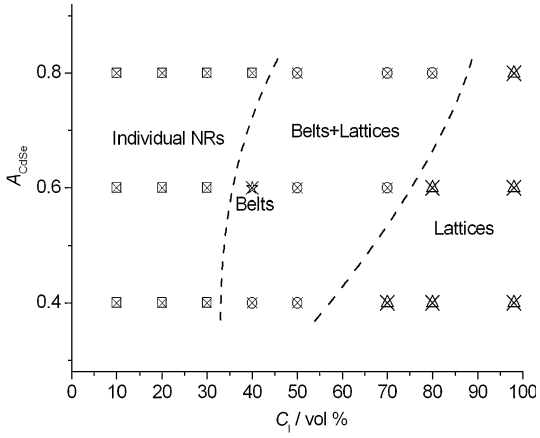

Figure 4. Phaselike diagram of the self-assembled structures of single-tip Au–CdSe NRs with varying A_{CdSe} in toluene/2-propanol. The star represents only belts. Concentration of NRs in the final solution: 0.8 mg mL^{-1} for NRs with A_{CdSe} = 0.4 and 0.6, and 1.0 mg mL^{-1} for NRs with A_{CdSe} = 0.8.

At a particular A_{CdSe}, with increasing content of 2-propanol in the mixed solvent, the NRs showed a stronger propensity to self-assemble in a side-by-side manner, thereby more efficiently screening interactions between the SLs and the solvent and minimizing the surface energy of the system. For example, at A_{CdSe} = 0.6 with increasing C_I the NRs underwent the following transitions: individual entities → belts → belts plus lattices → lattices. Importantly, at C_I = 98 vol% all three types of NRs underwent side-by-side assembly to form 2D lattices. These lattices formed close-packed standing NR arrays when they settled from the solution onto a solid substrate. In the lattices, the NRs have a hexagonal arrangement and inter-nanorod distance of about 2 nm, correlated with the thickness of the double layer of SLs.

For the same value of C_I, the formation of 2D lattices was favored at small values of A_{CdSe}. For example, for A_{CdSe} of 0.4 and 0.8 lattices formed at C_I of 70 and 98 vol%, respectively. We note that the A_{CdSe} value was largely determined by the length of the CdSe segment, which in the present work varied from about 7.5 to about 27.5 nm. (The width of the CdSe segment and the volume of the Au tips remained approximately constant.) Since the excluded volume of rods scales with the square of their length,[19] the onset of side-by-side attraction between the longer NRs required the addition of a larger amount of a nonsolvent.

We followed the formation and evolution of the 2D lattices for sample with A_{CdSe} = 0.4 at an NR concentration of 0.1 mg mL^{-1} and C_I = 50 vol% by combining TEM imaging and 90° DLS measurements. The images in Figure 5a and b show the growth of aggregates of NRs between 1 and 60 min after the addition of 2-propanol to a solution of NRs in toluene. Figure 5c shows the growth in scattering intensity at

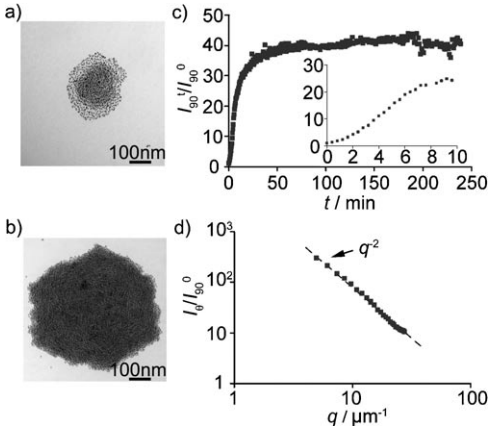

Figure 5. Evolution of lattices formed by NRs in 2-propanol/toluene at A_{CdSe} = 0.4, C_I = 50 vol%, and NR concentration of 0.1 mg mL^{-1}. TEM images of a representative NR lattice taken a) 1 and b) 60 min after addition of 2-propanol to the solution of NRs in toluene. c) Variation in I_{90}^t/I_{90}^0 with self-assembly time. The inset shows the evolution of the normalized scattering signal over the first 10 min. d) Log–log plot of I_θ/I_{90}^0 as a function of q from multiangle DLS measurements taken 200 min after addition of 2-propanol to the solution of NRs in toluene. The dashed line highlights the q^{-2} power law followed by the normalized scattered intensity.

90° (I^t_{90}/I^0_{90}). The scattering intensity for the first data acquisition ($t=0$, I^0_{90}) was very close to that of the mixture of toluene and 2-propanol, and this suggests that individual NRs were well-dispersed in solution. The inset in Figure 5c shows that association began within minutes after the solution was inserted into the light-scattering apparatus, in agreement with TEM-imaging experiments (Figure 5a) at 90°.

Similar behavior was observed for the growth of R_h^{app} monitored at 90° (Supporting Information). The plateau values in Figure 5c did not indicate the end of self-assembly, but rather that the objects have become too large to obtain meaningful data from scattering at 90°. Close to the end of the experiment (after 200 min) the scattered signal became noisy, which suggests that some of the large structures precipitated out of the solution. From the increase in the scattering intensity we infer that the NR arrays self-assembled in solution, and not on the substrate during drying.

Information about the shape of the self-assembled structures in solution was obtained from a multiangle light-scattering study carried out approximately 200 min after addition of 2-propanol to the solution of NRs in toluene, just prior to settling of large aggregates from the solution. Figure 5d presents a log–log plot of the normalized scattering intensity I_θ/I^0_{90} versus q, where I_θ is the scattering intensity measured at angle θ, and q the scattering vector, defined as $q=(4\pi n/\lambda)\sin^2(\theta/2)$, where n is the refractive index of the solvent, and λ the laser wavelength ($\lambda=632.8$ nm). The variation of I_θ/I^0_{90} vs. q^{-2}, plotted on the log–log graph, suggested that the lattice structures formed by the NRs in solution were two-dimensional, which was confirmed by fitting these data to the form factor of an infinitely thin circular disk (see Supporting Information).

In the standing arrays derived from 2D lattices, the NRs are arranged with the Au tips up or down (occasionally, we observed small clusters containing up to 5–8 NRs in the tip-up or tip-down orientation). Comprehensive analysis of 50 SEM images taken at an angle of 36° (Supporting Information) showed that the fraction of NRs assembled in the tip-up orientation was 55%.

In summary, we have demonstrated solution-based self-assembly of single-tip Au–CdSe NRs in a range of structures. In toluene, these NRs self-assemble to form multi-armed starlike structures and elongated objects. In solvent mixtures such as 2-propanol/toluene, beltlike planar structures and large superlattices are formed as a result of side-by-side association of the NRs. The propensity of the NRs to form 2D superlattices is favored at a large volume fraction of a nonsolvent for side ligands and a low volume fraction of CdSe in the NRs. The kinetics of aggregation of the NRs in solution was examined in light-scattering experiments. We found an unusual trend in the variation of the radius of gyration of the NR structures in the initial stages of self-assembly. For the first time, using multiangle DLS, we show that the evolving morphology of NR aggregates in solution is consistent with the structure imaged on a TEM grid.

Experimental Section

CdSe NRs stabilized with octadecylphosphonic acid (ODPA) and hexylphosphonic acid (HPA) were synthesized by using the method described elsewhere.[20–22] Three samples of NRs with average lengths of 7.5, 14.8, and 27.5 nm were synthesized by using injection temperatures of 300, 310, and 320 °C, respectively. The NRs were purified twice by precipitation with 2-propanol to remove residual precursors and excess ligands and redispersed in toluene. Then, an excess of dodecanethiol was added to the solution of NRs in toluene, to replace the ligands on the side faces of the NRs. After 4 h, the NRs were precipitated by adding 2-propanol to the solution of NRs in toluene, separated by centrifugation, and subsequently redispersed in toluene. The purification steps were repeated two or three times. (When dodecanethiol was not thoroughly removed from the solution, we were unable to grow Au tips on the ends of CdSe NRs). Selective growth of Au on a single tip of CdSe NRs was achieved by using the procedure reported by elsewhere,[15] with replacement of $AuCl_3$ with $HAuCl_4$. The reduction of $HAuCl_4$ on the tips of the CdSe NRs was carried out by using DDA in the presence of DDAB. The size of the Au tip was controlled by the amount of CdSe NR solution and the Au solution (see Supporting Information). After synthesis, single-tip Au–CdSe NRs were precipitated by adding 2-propanol to the reaction solution, separated by centrifugation, and redispersed in toluene.

Two types of self-assembly experiments were carried out. For spontaneous association in toluene, solutions of NRs with concentrations of 0.2–0.25 mg mL^{-1} were allowed to stand. Assembly was monitored over time by TEM, SEM, and, in separate experiments, by light scattering. These types of experiments led to tip-to-tip association. Samples for light scattering were more dilute (0.1 mg mL^{-1}), and prior to assembly they were filtered through Acrodisc CR 13 mm syringe filters with 0.45 μm PTFE membrane. Side-by-side association was triggered by adding different amounts (100–490 μL) of 2-propanol or *N*,*N*-dimethylformamide to NR solutions (10–400 μL) in toluene, so that the final concentration of NRs in the final solution was 0.8–1.0 mg mL^{-1}.

The self-assembled NR structures were imaged by TEM (Hitachi HD-2000 STEM) at 200 kV and SEM (S-5200) at 10 kV. A dilute solution of the NRs or a dispersion of self-assembled NRs was cast onto a carbon-coated copper grid and the solvent was evaporated. Multiangle dynamic light scattering (DLS) experiments were performed with a wide-angle light-scattering photometer from ALV, with a JDS Uniphase He–Ne laser ($\lambda_0=632.8$ nm, 35 mW) emitting vertically polarized light. The cells were placed into the ALV/DLS/SLS-5000 Compact Goniometer System and set in a vat of toluene, which matched the refractive index of the glass cells. The scattered light was detected by a Dual ALV-High Q.E. APD avalanche photodiode module, interfaced to the ALV-5000/EPP multiple tau digital. All measurements were carried out at room temperature. The apparent hydrodynamic radius R_h^{app} of the structure was deduced from the second-order cumulant analysis of the autocorrelation function. The absorption spectra of NRs changed during the assembly process. The decrease of the scattered signal due to the absorbance of the NRs at the laser wavelength of 633 nm was accounted for using the Beer–Lambert law (see the Supporting Information).

Received: August 6, 2010
Revised: January 21, 2011
Published online: April 19, 2011

Keywords: gold · light scattering · nanostructures · self-assembly · semiconductors

[1] R. Costi, A. E. Saunders, U. Banin, *Angew. Chem.* **2010**, *122*, 4996–5016; *Angew. Chem. Int. Ed.* **2010**, *49*, 4878–4897.

[2] P. D. Cozzoli, T. Pellegrino, L. Manna, *Chem. Soc. Rev.* **2006**, *35*, 1195 – 1208.
[3] R. Costi, A. E. Saunders, E. Elmalem, A. Salant, U. Banin, *Nano Lett.* **2008**, *8*, 637 – 641.
[4] H. Yu, M. Chen, P. M. Rice, S. X. Wang, R. L. White, S. Sun, *Nano Lett.* **2005**, *5*, 379 – 382.
[5] M.-C. Daniel, D. Astruc, *Chem. Rev.* **2004**, *104*, 293 – 346.
[6] L. Zhang, Y.-H. Dou, H.-C. Gu, *J. Colloid Interface Sci.* **2006**, *297*, 660 – 664.
[7] C. O'Sullivan, S. Ahmed, K. M. Ryan, *J. Mater. Chem.* **2008**, *18*, 5218 – 5222.
[8] P. D. Cozzoli, L. Manna, *Nat. Mater.* **2005**, *4*, 801 – 802.
[9] M. Hu, J. Chen, Z.-Y. Li, L. Au, G. V. Hartland, X. Li, M. Marquez, Y. Xia, *Chem. Soc. Rev.* **2006**, *35*, 1084 – 1094.
[10] A. Figuerola, I. R. Franchini, A. Fiore, R. Mastria, A. Falqui, G. Bertoni, S. Bals, G. Van Tendeloo, S. Kudera, R. Cingolani, L. Manna, *Adv. Mater.* **2009**, *21*, 550 – 554.
[11] A. Salant, E. Amitay-Sadovsky, U. Banin, *J. Am. Chem. Soc.* **2006**, *128*, 10006 – 10007.
[12] N. Zhao, K. Liu, J. Greener, Z. Nie, E. Kumacheva, *Nano Lett.* **2009**, *9*, 3077 – 3081.
[13] S. Deka, A. Falqui, G. Bertoni, C. Sangregorio, G. Poneti, G. Morello, M. De Giorgi, C. Giannini, R. Cingolani, L. Manna, P. D. Cozzoli, *J. Am. Chem. Soc.* **2009**, *131*, 12817 – 12828.
[14] G. Menagen, J. E. Macdonald, Y. Shemesh, I. Popov, U. Banin, *J. Am. Chem. Soc.* **2009**, *131*, 17406 – 17411.
[15] T. Mokari, C. G. Sztrum, A. Salant, E. Rabani, U. Banin, *Nat. Mater.* **2005**, *4*, 855 – 863.
[16] A. E. Saunders, I. Popov, U. Banin, *J. Phys. Chem. B* **2006**, *110*, 25421 – 25429.
[17] T. Mokari, E. Rothenberg, I. Popov, R. Costi, U. Banin, *Science* **2004**, *304*, 1787 – 1790.
[18] M. Schmidt, D. Nerger, W. Burchard, *Polymer* **1979**, *20*, 582 – 588.
[19] M. Rubinstein, R. H. Colby, *Polymer Physics*, Oxford Univ. Press, Oxford, **2003**.
[20] X. Peng, L. Manna, W. Yang, J. Wickham, E. Scher, A. Kadavanich, A. P. Alivisatos, *Nature* **2000**, *404*, 59 – 61.
[21] L. Manna, E. C. Scher, A. P. Alivisatos, *J. Am. Chem. Soc.* **2000**, *122*, 12700 – 12706.
[22] Z. A. Peng, X. Peng, *J. Am. Chem. Soc.* **2002**, *124*, 3343 – 3353.

